

01 Jan 2006

## Advanced Detection and Coding Techniques for Nonlinear Intersymbol Interference Cancellation in 40 Gb/S Systems

B. Vasic

I. B. Djordjevic

Vittal S. Rao

*Missouri University of Science and Technology*

Follow this and additional works at: [https://scholarsmine.mst.edu/ele\\_comeng\\_facwork](https://scholarsmine.mst.edu/ele_comeng_facwork)



Part of the [Electrical and Computer Engineering Commons](#)

---

### Recommended Citation

B. Vasic et al., "Advanced Detection and Coding Techniques for Nonlinear Intersymbol Interference Cancellation in 40 Gb/S Systems," *IEE Proceedings - Optoelectronics*, Institute of Electrical and Electronics Engineers (IEEE), Jan 2006.

The definitive version is available at <https://doi.org/10.1049/ip-opt:20050021>

This Article - Conference proceedings is brought to you for free and open access by Scholars' Mine. It has been accepted for inclusion in Electrical and Computer Engineering Faculty Research & Creative Works by an authorized administrator of Scholars' Mine. This work is protected by U. S. Copyright Law. Unauthorized use including reproduction for redistribution requires the permission of the copyright holder. For more information, please contact [scholarsmine@mst.edu](mailto:scholarsmine@mst.edu).

# Advanced detection and coding techniques for nonlinear intersymbol interference cancellation in 40 Gb/s systems

B. Vasic, I.B. Djordjevic and V.S. Rao

**Abstract:** To mitigate the fibre nonlinearities in high-speed transmission (at 40 Gb/s or higher), the use of maximum a posteriori probability (MAP) symbol decoding supplemented with iterative decoding is proposed. The MAP detector operates on the channel trellis to correct the corrupted data and to provide soft outputs processed further in an iterative decoder. Impressive performance improvement is demonstrated.

## 1 Introduction

Distortion of pulses due to dispersion and fibre nonlinearities (self-phase modulation, intrachannel four wave mixing and intrachannel cross-phase modulation) limits the amplifier span and consequently the total transmission distance of optical communication systems operating at high bit rates of 40 Gb/s and above. Moreover, high-speed optical transmission systems operating at 40 Gb/s or higher are severely limited by intrachannel nonlinearities such as intrachannel four-wave mixing and intrachannel cross-phase modulation. Previous work in intersymbol interference (ISI) reduction at lower bit rates has involved the use of equalisation [1] and nonlinear cancellation [2]. Linear equalisers cannot handle nonlinear effects, and the cancellation technique does not take into account the effect of post-cursor ISI. Other approaches such as the use of line coding [3] have also been proposed. Some efforts have also been made on the design of 'constrained maximum likelihood detection' schemes [4], but these schemes, although theoretically optimal, do not perform as well in practice because of the simplifications made in order to reduce the system complexity.

The turbo-equalisation, proposed by Douillard *et al.* [5], performs very well when the channel is known to the receiver, which is not the case in optical transmission. The turbo-equalisation-like schemes have been considered intensively for a variety of applications: wireless communications [6], CDMA [7], magnetic recording [8] and so on. However, no attempt has been made (up to the best of our knowledge) to apply this technique in high-speed optical transmission.

To improve the data transmission performance in systems heavily degraded by fibre nonlinearities and dispersion, we propose a scheme that combines nonlinear ISI cancellation and error control coding. Our ISI cancellation scheme uses maximum a posteriori probability (MAP) symbol

decoding based on Bahl-Cocke-Jelinek-Raviv (BCJR) algorithm [9], whereas the error control code is the affine geometry (AG) based low-density parity-check (LDPC) code [10–12].

To investigate nonlinear ISI at high bit rates, we use a simulator that takes into account the effects of the optical and electrical components employed in the system. Through simulations, the channel behaviour is recorded and compiled in the form of a trellis. MAP decoding is then used to counter the nonlinear ISI and a dramatic performance improvement is shown. The scheme proposed can operate in the regime of very strong intrachannel nonlinearities where other equalisation schemes are not able to operate. The scheme proposed is also an excellent candidate for a 40 Gb/s upgrade over existing 10 Gb/s infrastructure.

## 2 Detection and decoding

Bahl *et al.* [9] proposed a (MAP) decoding algorithm that can be used for any kind of finite state machine-driven sequence in general. As opposed to the Viterbi algorithm [13], which is a maximum likelihood sequence estimation (MLSE) method, the BCJR algorithm is an optimal detection method that minimises symbol error probability.

Many experiments have been carried out in applying this algorithm, not only to decode codes that can be described as a trellis, but also in the detection of data sent over channels with memory. Previous work has shown that BCJR can be used to successfully counter the effects of ISI on magnetic channels [8]. The output of the channel is described by a trellis and BCJR works on this trellis to correct the corrupted data. A significant benefit of using the BCJR algorithm is that it provides reliable soft values at the output processed further by an iterative decoding scheme. In our research, we used the BCJR algorithm to tackle the nonlinear ISI present in the optical channel. The trellis that the BCJR algorithm works with is, in fact, a dynamic model of the optical channel.

Suppose that a dispersion map is chosen so that each bit is influenced by three neighbouring bits from either side. The nonlinear ISI patterns are determined by simulations in the following way. A total of 128 7-bit patterns were sent through the channel and the outputs (for the central bit) were observed. These outputs were tabulated to form the

**Table 1: Illustration of determining the nonlinear ISI pattern**

Previous pattern	Present pattern	Central bit (label)
000 0 001	000 0 010	0.08165076
000 0 001	000 0 011	0.08207725
000 0 010	000 0 100	0.36531320
000 0 010	000 0 101	0.47133360

trellis. As an illustration, signal values for some data patterns are shown in Table 1.

A set of triples (previous pattern, next pattern and channel output) uniquely defines a finite state machine on which BCJR operates. A state transition diagram unwraps in time to form a trellis. Fig. 1 shows one stage of the structure of the trellis used. This trellis has 128 states,  $(s_1, s_2, s_3, \dots, s_{128})$ , and each state represents a 7-bit pattern. Each vertical column represents the various states in the system at a given point in time, whereas the labelled edges represent possible transitions. Neighbouring columns thus represent consecutive points in time. When the system is at state  $s_1$  (bit pattern 0000000), if the next bit is ‘0’ it stays in state  $s_1$ , else it goes to state  $s_2$  (bit pattern 0000001). No other transitions are allowed from state  $s_1$ . Similarly, there are two possible transitions from each state in the trellis. A labelled edge is assigned to each allowed transition. A label is the sample value, at the output of the electrical filter, corresponding to the central bit (Table 1).

Given  $s'$  is the previous state,  $s$  is the present state and  $y = (y_1, y_2, \dots, y_n)$  the received codeword. The BCJR algorithm sweeps the trellis in the forward direction to find the probabilities  $\alpha_k(s)$  through ‘forward recursion’ as

$$\alpha_k(s) = \sum_{s'} \gamma_k(s', s) \alpha_{k-1}(s')$$

and in the backward direction to find the probabilities  $\beta_k(s)$  through ‘backward recursion’ as

$$\beta_{k-1}(s') = \sum_s \beta_k(s) \gamma_k(s', s)$$

where  $\gamma_k(s', s)$  is given by

$$\gamma_k(s', s) = p(s, y_k | s')$$

and it is determined from simulations. The initial values are set to

$$\alpha_0(s) = \begin{cases} 1, & s = 0 \\ 0, & s \neq 0 \end{cases} \quad \text{and} \quad \beta_k(s) = \begin{cases} 1, & s = 0 \\ 0, & s \neq 0 \end{cases}$$

Given that the transmitted codeword is denoted by  $U = (u_1, u_2, \dots, u_n)$ , the log-likelihood ratio used as soft input (denoting the bit reliability) in the iterative decoder

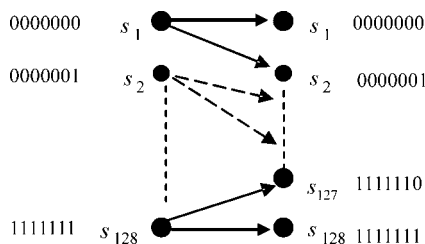


**Fig. 1** Snapshot of the trellis used by BCJR

is calculated as

$$L(u_k) = \log \frac{\sum_{U_1} \alpha_{k-1}(s') \gamma_k(s', s) \beta_k(s)}{\sum_{U_0} \alpha_{k-1}(s') \gamma_k(s', s) \beta_k(s)}$$

where  $U_1$  denotes the set of pairs  $(s', s)$  for the state transitions that correspond to the  $u_k = 1$  and  $U_0$  is similarly defined for  $u_k = 0$ . In our case, instead of using  $L(u_k)$  to make the decision, it is used as the soft input to the iterative LDPC decoder.

The second component of our scheme is an LDPC code. The main idea is to use the BCJR algorithm to partially cancel nonlinear ISI and reduce BER to  $10^{-3}$  or  $10^{-4}$  and then feed soft information obtained from the BCJR algorithm into iterative decoder of the LDPC code. We consider the LDPC codes constructed using AG. These codes can have large minimum distances and perform very well in optical communication channels [10]. For more details on the AG LDPC codes and the employed min-sum LDPC decoding algorithm, the interested reader is referred to our previous article [10].

The choice of AG codes can be justified by the fact that in high-speed optical transmission, it is important to keep the detector and decoder complexity low and obtain the largest coding gain possible. Therefore, even though highly irregular LDPC codes, designed by EXIT charts analysis [14], show an excellent performance on an additive white Gaussian channel model, they are not applicable because of the high complexity of the encoder. In contrast, AG codes have cyclic or quasi-cyclic structure of both parity-check and generator matrices [15] and excellent bit-error rate (BER) performance in optical channels [10].

### 3 Simulator and map description

To investigate nonlinear ISI in high-speed channels, we developed a realistic simulation model that takes into account impairments found in practical systems. We consider the single channel transmission at 40 Gb/s, as our focus is intrachannel ISI.

As the intention is to show that BCJR can salvage data even in situations where the distortion is very high, a non-optimal (non-slope matched) dispersion map, Fig. 2, is chosen. The map consists of  $N$  spans of standard single-mode fibre (SMF) and dispersion compensating fibre (DCF) sections, followed by an amplifier to compensate the fibre losses in both sections. The modulator is a non-return-to-zero (NRZ) modulator composed of a Mach-Zehnder (MZ) laser diode, a modulator (with a driver) and a pseudo-random bit sequence (PRBS) generator. When the bit stream is encoded, an LDPC encoder is also present.

The receiver observed, Fig. 3, is composed of an optical filter, a p-i-n photodiode, an electrical filter and a sampler, followed by a BCJR detector and an MP decoder.

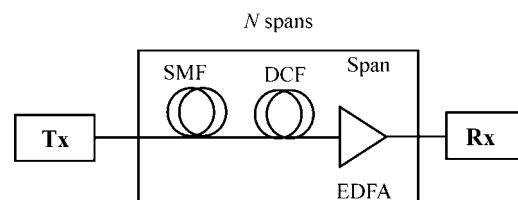


**Fig. 2** Dispersion map under study

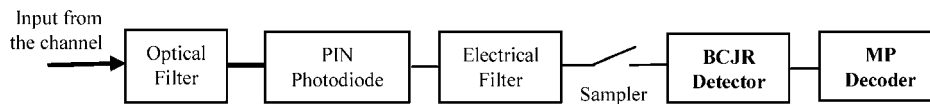


**Fig. 3** Receiver model

The propagation of a signal through the transmission media is modelled by the nonlinear Schrödinger equation [11]

$$\frac{\partial A}{\partial z} = -\frac{\alpha}{2}A - \frac{i}{2}\beta_2 \frac{\partial^2 A}{\partial T^2} + \frac{\beta_3}{6} \frac{\partial^3 A}{\partial T^3} + i\gamma|A|^2 A$$

where  $z$  is the propagation distance along the fibre, relative time  $T = t - z/v_g$  gives a frame of reference moving at the group velocity  $v_g$ ,  $A(z, T)$  is the complex field amplitude of the pulse,  $\alpha$  is the attenuation coefficient of the fibre,  $\beta_2$  is the group velocity dispersion (GVD) coefficient,  $\beta_3$  is the second-order GVD,  $\gamma$  is the nonlinearity coefficient giving rise to Kerr effect nonlinearities: self-phase modulation, intrachannel cross-phase modulation and intrachannel four-wave mixing. In short, we use a system that takes into account a number of the natural effects that the light travelling through a fibre communication system would face. We take care of modulation, extinction ratio, realistic models of transmitter, optical filter and electrical filter, ISI, Kerr nonlinearities, amplified spontaneous emission (ASE) noise and dispersion effects (GVD and second-order GVD).

#### 4 Performance analysis

To illustrate the strength of the proposed method, we will consider the systems with bad dispersion maps and show that even in this case, when other techniques fail, our method still provides a significant gain and can be used for 40 Gb/s systems upgrade over existing 10 Gb/s infrastructure. The simulated system is comprised of six spans of 120 km of SMF, followed by 20.4 km of DCF. The dispersion map consists of an SMF section, followed by a DCF section to compensate GVD, and an Erbium-doped fibre amplifier (EDFA) to compensate the fibre losses of both sections. The  $Q$ -factor is additionally decreased by noise loading. The SMF attenuation coefficient, dispersion, dispersion slope, nonlinear refractive index and effective cross sectional area are set to 0.21 dB/km, 17 ps/nm km, 0.065 ps/nm<sup>2</sup> km,  $2.6 \times 10^{-20}$  m<sup>2</sup>/W and 80  $\mu\text{m}^2$ , respectively. Corresponding DCF parameters are 0.5 dB/km, -100 ps/nm km, 0.33 ps/nm<sup>2</sup> km,  $2.6 \times 10^{-20}$  m<sup>2</sup>/W

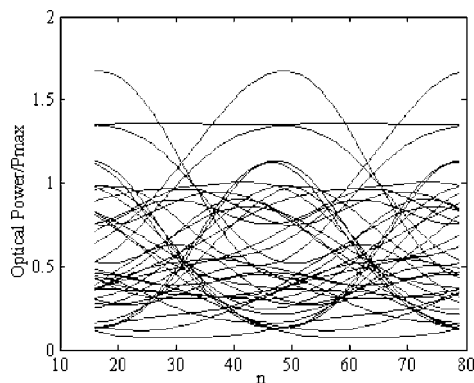


**Fig. 4** Output electrical eye-diagram for  $Q = 3.02$  dB (32 samples/pulse)

and 30  $\mu\text{m}^2$ . The launched power is set to 0 dBm. For this configuration, we found that the data were severely distorted because of nonlinear ISI. Fig. 4 shows the output eye-diagram of the electrical signal. This eye-diagram is completely closed and indicates that the uncoded system performance will be severely limited by the nonlinear ISI experienced in the channel.

As described in the preceding section, a channel trellis (on which the BCJR algorithm operates) was created using the simulation outputs. We found that most of the ISI was contributed by the 3 bits on either side of an observed bit. (As the number of links increases, more bits need to be considered.) The accuracy was not improved significantly by a small increase in this number. To create the trellis, the various 7 bit patterns were passed through the fibre and their output values were recorded.

The soft likelihood values at the BCJR algorithm output were fed to the iterative decoder that outputs hard decision bit values after three iterations. An LDPC (1056, 813) code based on AG (2,32) is employed in simulations.

Simulation results are shown in Fig. 5. The results correspond to the channel centred at 1552.524 nm. To reduce the decoding delay, no iteration between LDPC decoder and BCJR is performed and the number of iterations in LDPC decoder is set to six. Because of the BER floor of an uncoded system, the  $Q$ -factor is estimated by the following formula:  $Q = (\mu_1 - \mu_0)/(\sigma_1 + \sigma_0)$ , where  $\mu_i$  and  $\sigma_i$  ( $i = 1, 0$ ) are, respectively, mean values and standard deviations associated with 1 and 0 bits. The influence of overhead is not taken into account in simulations. From the graph, we see that the BCJR algorithm on its own improves the system performance until a BER of  $10^{-4}$  is reached but levels off after this point. This is because the input to the BCJR algorithm, which is a trellis, is an approximation of a nonlinear process. The accuracy of this model is diminished by two factors. First, no more than 3 bits on either side of a given bit are considered, and second, the nonlinear effects in the channel are wavelength dependent. Beyond a certain point, the BCJR algorithm is unable to improve the

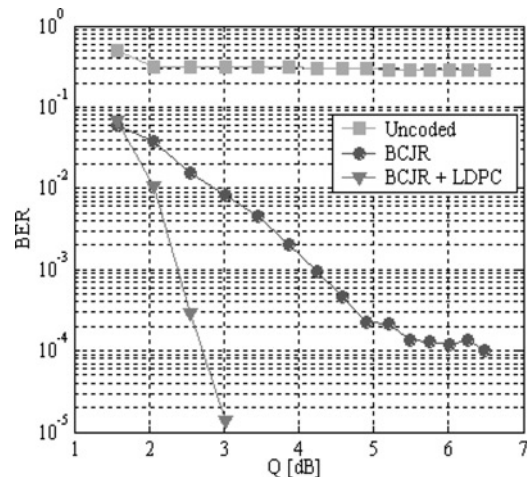


**Fig. 5** Performance curves

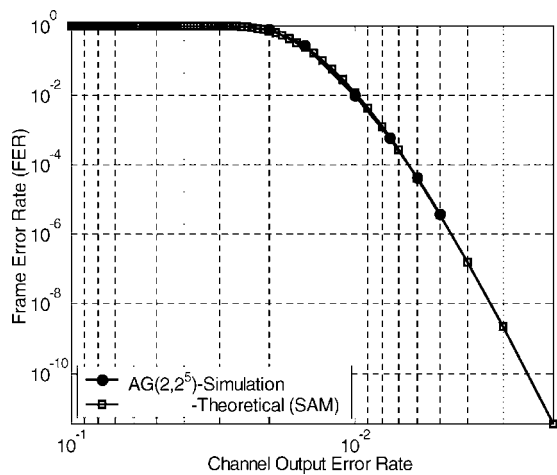


**Fig. 6** Semi-analytic method (SAM) for frame-error rate analysis of AG codes for hard decision decoding using Gallager B algorithm (as described in [22])

system performance as we are limited by initial assumptions.

Iterative decoding, in contrast, has no such limitation. So, as expected, we see a large improvement in system performance. An error floor occurs at the  $Q$ -factor at which the BCJR algorithm's performance starts levelling off. We have recently shown [16–18] (Fig. 6) that the AG-based codes do not exhibit an error floor in the region of interest for fibre-optics communications. If we extrapolate the triangle curve from Fig. 5, we see that BER below  $10^{-13}$  is reached before the forward error correction (FEC) threshold, which is for applied LDPC code and soft decoding in the order of  $10^{-2}$  [10], well above the BCJR BER error floor.

It should be also noticed that an iterative decoding without the BCJR algorithm is unable to improve the system performance. Numerous errors caused by the ISI quickly overwhelm the correction capability of the LDPC code. The system is operating above the 'FEC threshold', and until the MAP decoding brings the operating point below this threshold, forward error correction codes are not able to provide any gain. Another way to observe these results is to consider the BCJR curve as the BER performance of an uncoded system with perfectly cancelled nonlinear ISI. At a BER of  $10^{-3}$ , the BCJR + LDPC system gives 1.9 dB of coding gain over this equivalent uncoded system. Earlier results [19] have shown that LDPC codes alone can provide similar performance improvement in systems operating at 10 Gb/s.

The overall coding gain is infinitely large as the uncoded system reaches error floor at a BER of 0.3. Further performance improvement is possible if the channel is modelled by trellis with larger number of states.

Notice that other techniques for suppression of intrachannel nonlinearities [19], based on Volterra series method or MLSE, do not provide soft outputs required for soft iterative (turbo or LDPC) decoding, and as such are not discussed here. The Volterra series nonlinear equalisation technique used to improve the performance in a duobinary modulation scheme in [20] also suffers from error propagation due to the nonlinear feedback.

## 5 Conclusion

In conclusion, MAP detection supplemented with iterative decoding is able to achieve impressive performance

improvement in systems heavily degraded by ISI because of fibre nonlinearities and dispersion. The fact that there is much room for research in the field of detection and decoding for nonlinear channels opens doors for the optimism that even larger coding gains are possible. The uncoded BER exhibits the error floor. With one in 3 bits being in error, the system is unusable. Even encoding the data before transmission will not mitigate the errors if data rate is to be kept reasonable. Because of the high complexity of the BCJR algorithm for high-speed implementation, a simplified version of it, namely soft output Viterbi algorithm [21], is more likely to be of interest for practical implementations. Notice also that the trellis in Fig. 1 is highly regular with only two transitions from every state, and the same structure may be reused at different levels.

## 6 Acknowledgment

This work is supported by the NSF under grant ITR 0325979 and CCR 0208597.

## 7 References

- Winters, J.H.: 'Equalization in coherent lightwave systems using a fractionally spaced equalizer', *J. Lightwave Technol.*, 1989, **7**, pp. 813–815
- Kasturia, S., and Winters, J.H.: 'Techniques for high-speed implementation of nonlinear cancellation', *IEEE J. Sel. Areas Commun.*, 1991, **9**, pp. 711–717
- Swenson, N.L., and Cioffi, J.M.: 'Coding techniques to mitigate dispersion-induced ISI in optical data transmission'. Proc. IEEE Int. Conf. Commun., 1990, pp. 468–472
- Winters, J.H., and Kasturia, S.: 'Constrained maximum-likelihood detection for high-speed fiber-optic systems'. Proc. IEEE GLOBECOM, December 1991, pp. 1574–1579
- Douillard, C., Jezequel, M., Berrou, C., Picart, A., Didier, P., and Glavieux, A.: 'Iterative correction of intersymbol interference: turbo equalisation', *Eur. Trans. Telecommun.*, 1995, **6**, pp. 507–511
- Song, S., Singer, A.C., and Sung, K.-M.: 'Soft input channel estimation for turbo equalisation', *IEEE Trans. Signal Process.*, 2004, **52**, pp. 2885–2894
- Wang, X., and Poor, H.: 'Iterative (turbo) soft interference cancellation and decoding for CDMA', *IEEE Trans. Commun.*, 1999, **47**, pp. 1046–1061
- Kurkoski, B.M., Siegel, P.H., and Wolf, J.K.: 'Joint message-passing decoding of LDPC codes and partial-response channels', *IEEE Trans. Inf. Theory*, 2002, **48**, pp. 1410–1422
- Bahl, L.R., Cocke, J., Jelinek, F., and Raviv, J.: 'Optimal decoding of linear codes for minimizing symbol error rate', *IEEE Trans. Inf. Theory*, 1974, **IT-20**, (2), pp. 284–287
- Djordjevic, I.B., and Vasic, B.: 'Performance of affine geometry low-density parity-check codes in long-haul optical communications', *Eur. Trans. Telecommun.*, 2004, **15**, pp. 477–483
- Djordjevic, I.B., Sankaranarayanan, S., and Vasic, B.: 'Projective plane iteratively decodable block codes for WDM high-speed long-haul transmission systems', *IEEE/OSA J. Lightwave Technol.*, 2004, **22**, pp. 695–702
- Vasic, B., Kurtas, E., and Kuznetsov, A.: 'LDPC codes based on mutually orthogonal Latin rectangles and their application in perpendicular magnetic recording', *IEEE Trans. Magn.*, 2002, **38**, (5), pp. 2346–2348
- Viterbi, A.J.: 'Error bounds for convolutional codes and an asymptotically optimum decoding algorithm', *IEEE Trans. Inf. Theory*, 1967, **IT-13**, pp. 260–269
- Ten Brink, S., Kramer, G., and Ashikhmin, A.: 'Design of low-density parity-check codes for modulation and detection', *IEEE Trans. Commun.*, 2004, **52**, pp. 670–678
- Kou, Y., Lin, S., and Fossorier, M.P.C.: 'Low-density parity-check codes based on finite geometries: a rediscovery and new results', *IEEE Trans. Inf. Theory*, 2001, **47**, pp. 2711–2736
- Djordjevic, I.B., Sankaranarayanan, S., Chilappagari, S.K., and Vasic, B.: 'Low-density parity-check codes for 40 Gb/s optical transmission systems', *IEEE J. Sel. Top. Quantum Electron.*, submitted for publication

- 17 Chilappagari, S.K., Sankaranarayanan, S., and Vasic, B.: 'Error floors of LDPC codes on binary symmetric channel'. Int. Conf. on Communications, ICC 2006, Istanbul, Turkey, June 2006, accepted for publication
- 18 Vasic, B., Chilappagari, S.K., and Sankaranarayanan, S.: 'Error floors of LDPC codes on binary symmetric channel'. IEEE Comm. Theory Workshop, Park City, UT, June 13–15, 2005
- 19 Vasic, B., and Djordjevic, I.B.: 'Low-density parity check codes for long-haul optical communication systems', *Photonics Technol. Lett.*, 2002, **14**, pp. 1208–1210
- 20 Xia, C., and Rosenkranz, W.: 'Performance enhancement for duobinary modulation through nonlinear electrical equalisation'. Proc. ECOC, 2005, 2005, Vol. 2, pp. 257–358
- 21 Hagenauer, J., and Hoher, P.: 'A Viterbi algorithm with soft decision outputs and its applications'. Proc. IEEE GLOBECOM, November 1989, pp. 1680–1686
- 22 Gallager, R.: 'Low-density parity-check codes', *Trans. Inf. Theory*, 1962, pp. 21–28